

Transient reshaping of intersubband absorption spectra due to hot electrons in a modulation-doped multiple-quantum-well structure

R. J. Bäuerle and T. Elsaesser

Physik Department E 11 der Technischen Universität München, D-8000 München 2, Federal Republic of Germany

H. Lobentanzer,* W. Stolz,† and K. Ploog

Max-Planck-Institut für Festkörperforschung, D-7000 Stuttgart 80, Federal Republic of Germany

(Received 7 July 1989)

The intersubband absorption spectrum of hot electrons is studied in a $\text{Ga}_{0.47}\text{In}_{0.53}\text{As}/\text{Al}_{0.48}\text{In}_{0.52}\text{As}$ multiple-quantum-well structure by picosecond infrared spectroscopy. The bandwidth of the transition between the $n=1$ and $n=2$ conduction subbands increases from 7 to 13 meV for a rise of the transient carrier temperature from 10 to 350 K. This broadening relaxes with carrier cooling on a time scale of approximately 100 ps. The different dispersion of the two subbands and the broad distribution function of hot electrons result in a temperature-dependent bandwidth of the spectrum. Theoretical calculations account quantitatively for our data.

Intersubband absorption of electrons in layered semiconductors has been studied in a variety of multiple-quantum-well (MQW) structures and superlattices.¹⁻⁵ The spectral position and the strength of the absorption lines depend on the width and the doping concentration of the quantum wells (QW's). These features make n -doped heterostructures promising for photodetectors sensitive in the infrared spectral range. Investigations of the intersubband excitation and relaxation processes are a prerequisite for application. Here hot carrier phenomena play a central role.

Recently, we have studied the intersubband absorption and scattering of electrons in an n -type modulation-doped $\text{Ga}_{0.47}\text{In}_{0.53}\text{As}/\text{Al}_{0.48}\text{In}_{0.52}\text{As}$ MQW structure.⁵⁻⁷ A strong absorption line connected with transitions from the $n=1$ to the $n=2$ conduction subband was found around 150 meV for a QW thickness of 8.2 nm. The spectral width of the band increases from 7 to 12 meV for a rise of the sample temperature from 10 to 300 K, whereas the oscillator strength of $f \approx 20$ and the spectral position remain nearly unchanged.

Several mechanisms contribute to the total linewidth: (i) The scattering time of electrons from the $n=2$ to the $n=1$ subband lies in the range between 0.5 and 3 ps for the ternary MQW structure⁶ and may result in a certain lifetime broadening of the absorption spectrum; (ii) the different dispersion of the conduction subbands in k space leads to a k -dependent energy of the transition and a temperature-dependent broadening; and (iii) inhomogeneities of the QW thickness contribute to the total linewidth.

A separation of the various contributions and their temperature dependence is not possible in steady-state experiments. Time-resolved measurements, where hot carriers are investigated in a MQW structure at low lattice temperatures, should allow a discrimination of the effects due to electron and to lattice temperature. In this paper, we study, for the first time, intersubband absorption spectra of hot electrons on the picosecond time scale. The spectra change significantly with the time-dependent carrier tem-

perature. The different effective masses and nonparabolicities of the two subbands are essential for the transient change of absorption.

The n -type modulation-doped MQW structure investigated in our experiments was grown by molecular-beam epitaxy. The sample consists of 50 $\text{Ga}_{0.47}\text{In}_{0.53}\text{As}$ quantum wells separated by $\text{Al}_{0.48}\text{In}_{0.52}\text{As}$ barriers and is grown on a (100) InP substrate. The thickness of the QW's and the barriers amounts to 8.2 and 23.4 nm, respectively. The electron density in each quantum well has a value of $4.2 \times 10^{11} \text{ cm}^{-2}$.

The picosecond measurements are based on the following pump and probe scheme: A small number of hot electron-hole pairs is generated by interband excitation from the valence to the conduction bands. The electrons are rapidly scattered to the lowest ($n=1$) conduction band, thermalize with the electrons present by doping, and form a hot electron distribution. The delayed probe pulses, which are tunable in the spectral range of the transition from the $n=1$ to the $n=2$ conduction band, monitor changes of this absorption line.

Excitation pulses at 1.17 eV are generated in a mode-locked Nd:yttrium aluminum garnet (YAG) laser system. The pulse duration is 22 ps. Tunable pulses in the wavelength range from 4 to 9.5 μm (0.3 to 0.13 eV) are produced by parametric frequency conversion. The output of the Nd:YAG laser and of a near-infrared dye laser is mixed in a nonlinear AgGaS_2 crystal to generate the difference frequency.⁸ The duration and the spectral bandwidth of the infrared pulses amount to 8 ps and 1 meV, respectively. The polarization vector of the probe pulses lies in the plane of incidence and the sample is oriented under the Brewster angle in the infrared beam. In this geometry, a small component (approximately 10%) of the probe light interacts with the intersubband dipole moment, which has a direction perpendicular to the layers of the MQW system. All measurements are performed with a lattice temperature of 10 K.

The intersubband absorption spectra of the electrons are presented in Fig. 1. The solid line represents the

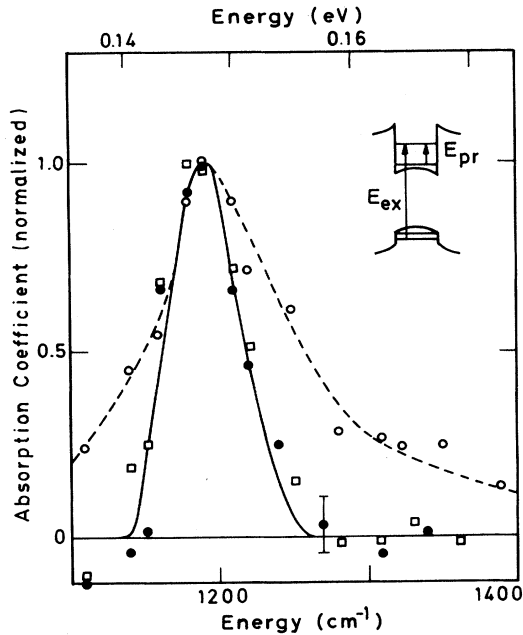


FIG. 1. Intersubband absorption spectra of the n -doped MQW structure. The normalized absorption coefficient is plotted vs the photon energy E_{pr} . The spectrum of the unexcited sample was measured in a steady-state infrared spectrometer (solid line) and by tunable picosecond pulses (points). The spectral envelope changes after excitation of hot electrons by a picosecond pulse at $E_{ex}=1.17$ eV (the circles and the dashed line indicate data for a delay time of 20 ps). Squares represent the spectrum at a delay time of 100 ps.

steady-state spectrum with an oscillator strength of $f=21$, as observed in a standard infrared spectrometer.⁵ The same result is found with the tunable picosecond pulses (points). Strong changes of the band are observed after picosecond excitation of hot additional carriers by the pulse at 1.17 eV. Approximately 2×10^{11} electron-hole pairs per cm^2 with an excess energy of 280 meV are created. The circles (dashed line) give the normalized transient spectrum measured at a delay time of 20 ps between pump and probe pulses, when the excess electrons exclusively populate the $n=1$ conduction subband.⁶ The absorption line broadens by a factor of approximately 2 and shows a slight shift of the center to higher energies. The absolute value of the absorption coefficient at 148 meV rises by 30%.

The changes of the spectral envelope decay within 100 ps. The spectrum measured at that delay time has a shape close to the original band (squares in Fig. 1). The absolute absorption coefficient after 100 ps still exceeds the steady value by 20% due to the excess electrons generated by the excitation pulse.

The kinetics of the absorption change was studied with probe pulses of fixed frequency. As examples, we present measurements at $E_{pr}=165$ meV [Fig. 2(a)] and 148 meV [Fig. 2(b)] on the high-energy side and at the maximum of the original line, respectively. The change of absorption $\Delta A = -\ln(T/T_0)$ is plotted versus the delay time between pump and probe pulses (T_0 and T represent the

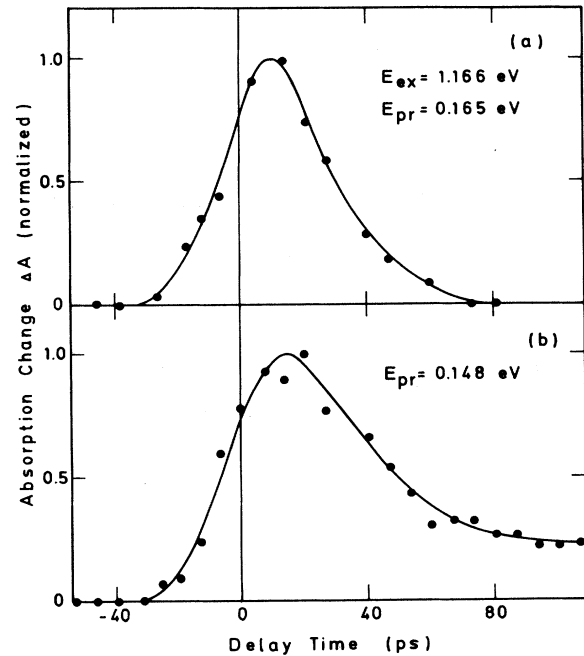


FIG. 2. Time-dependent change of the intersubband absorption for two photon energies of the probe pulses. The normalized absorption change $\Delta A = -\ln(T/T_0)$ is plotted as a function of delay time between the excitation (E_{ex}) and the probe pulses (E_{pr}); T_0 and T represent sample transmission before and after excitation. (a) Transient absorption at $E_{pr}=0.165$ eV above the original absorption band (cf. Fig. 1). (b) Change of absorption at the maximum of the original line ($E_{pr}=0.148$ eV). The long-lived residual signal is due to the generated excess electrons. This contribution decays by recombination with a time constant of 250 ps.

transmission of the sample before and after excitation). At $E_{pr}=165$ meV, where the initial absorption is zero, we find a rapid rise of the signal, which decays within 70 ps. A similar fast kinetics is observed at $E_{pr}=135$ meV below the original band (not shown in Fig. 2). These results directly demonstrate the transient change of spectral bandwidth. The kinetics of spectral broadening is in good agreement with the time-dependent cooling behavior measured in the same MQW sample for similar excitation density and excess energy.^{6,7} At $E_{pr}=148$ meV, a long-lived contribution to the signal is found in addition to the fast component [Fig. 2(b)]. This second component decays by recombination of the excess carriers with a time constant of 250 ps.

After the intersubband relaxation of the excess electrons within less than 3 ps, band filling leads to a strong bleaching of the absorption spectrum at energies close to the band gap between the $n=1$ valence and conduction band around 0.87 eV. The transient absorption spectra in this region directly reveal the momentary carrier distribution function.⁷ This technique gives for the present experiments a density $N_{ex} \approx 2 \times 10^{11} \text{ cm}^{-2}$ of excess carriers and a momentary electron temperature of $T_c = 350$ K for a delay time of 20 ps, where the transient intersubband spectrum of Fig. 1 is recorded.

We now discuss the transient reshaping of the intersubband absorption spectrum. Two broadening mechanisms have to be considered in detail, namely the change of the intersubband scattering time with temperature and the influence of subband dispersion on the line shape. The contribution of sample inhomogeneities to the linewidth is expected to be independent of the carrier temperature.

The energy of the intersubband transition in our MQW system markedly exceeds that of the longitudinal-optical (LO) phonons. As a result, interaction with LO phonons is the main intersubband scattering process of electrons with a lifetime of the upper subband between 0.5 and 3 ps.⁶ The total electron-phonon scattering rate is the sum of phonon emission and absorption processes proportional to $N_q + 1$ and N_q , respectively, where N_q is the population probability of the LO phonon branch (q represents the phonon wave vector).⁹ The equilibrium phonon density depends on the lattice temperature T_L , but not on the carrier temperature T_c . In the present experiments, T_L has a constant value of 10 K. Thus, only the creation of excess LO phonons by the initial fast intersubband scattering could lead to a time-dependent rise of N_q in the relevant q interval and a corresponding change of the intersubband scattering time. The latter would alter the lifetime broadening of the spectrum. A quantitative estimate of this effect taking into account the excitation density, the excess energy of the electron-hole pairs, and the region in q space, where phonons are emitted, gives a change of the linewidth, which amounts to less than 10% of the steady-state value found at 10 K. Therefore, this mechanism cannot explain the strongly broadened spectra found in our measurements.

Next, we consider consequences of the different dispersion of the subbands with k_p , the wave vector parallel to the layers of the MQW structure. The different effective masses and nonparabolicities of the two conduction subbands result in a k_p -dependent energy ΔE_s of the intersubband transition. At low carrier temperatures, the electrons populate states at small k_p values and ΔE_s is determined by the separation of the subbands around $k_p = 0$. The electronic distribution function at the high transient temperatures occurring in the picosecond measurements extends over a larger k_p interval. Here different values of ΔE_s contribute to the spectrum resulting in a distinct broadening of the absorption line.

The electron density in the $n=1$ subband increases by picosecond excitation. The change of carrier concentration leads to a shrinkage of the $n=1$ band gap by renormalization.¹⁰ This effect is accompanied by a shift of the intersubband spectrum to higher energies (increasing ΔE_s), since the $n=2$ conduction subband is only weakly changed in energy by the carriers in the $n=1$ system.¹¹ In the following, we calculate intersubband absorption spectra taking into account subband dispersion and band-gap renormalization.

The theoretical description of the electronic band structure in two dimensions is based on an approach where parabolic subbands are determined self-consistently and nonparabolicity as well as spin-orbit terms are treated by perturbation theory.^{12,13} The carrier motion in the layered system is separated in a first part parallel to the plane of

the QW's, which is characterized by the wave vector k_p , and a second component perpendicular to the layers (k_z). The dispersion of electronic energy is calculated up to fourth order in k and averaged over the two orientations of electron spin. The small warping of the band structure is neglected. The energy E_{cn} ($n=1,2$) of the carriers at $k_p=0$ is determined by the two-dimensional confinement in the QW's. We calculate $E_{c1}=61$ meV and $E_{c2}=205$ meV for a QW thickness of 8.2 nm. Around $k_p=0$, the subbands are characterized by an effective mass m_n ($n=1,2$). A value of $m_1=0.049m_0$ (m_0 represents the free electron mass) is calculated for the lowest subband, in good agreement with the effective mass measured by cyclotron resonance.¹⁴ The effective mass of the $n=2$ subband is larger and has a value of $m_2=0.061m_0$. The dispersion at larger values of k_p significantly deviates from a parabolic shape. We find nonparabolicity factors of $\alpha_1=0.98$ eV⁻¹ and $\alpha_2=0.78$ eV⁻¹ for the two subbands.¹²

The temperature-dependent renormalization of the $n=1$ band gap is calculated from the formalism presented in Ref. 10. A shift of 11 meV is obtained for an electron density of 4.2×10^{11} cm⁻² at 10 K.

The intersubband absorption coefficient $\alpha_{IS}(h\nu)$ at the energy $h\nu$ is given by

$$\alpha_{IS}(h\nu) = C \int d^2k_p f(E_1) [1 - f(E_2)] L(h\nu - (E_2 - E_1)).$$

$f(E_1)$ and $f(E_2)$ are the Fermi distribution functions of electrons in the two subbands depending on the energies $E_1(k_p)$ and $E_2(k_p)$, the Fermi levels, and the carrier temperature T_c . The function $f(E_2)$ is close to zero for our experimental conditions. The spectral profile $L(h\nu - [E_2(k_p) - E_1(k_p)])$, which is independent of T_c , is introduced to account for the spectral width due to the sample inhomogeneities and to the finite lifetime of the $n=2$ subband. It should be noted that the shape and the total width of the intersubband spectrum are determined by the profile $L(h\nu)$ and the distribution functions $f(E_{1,2})$. C

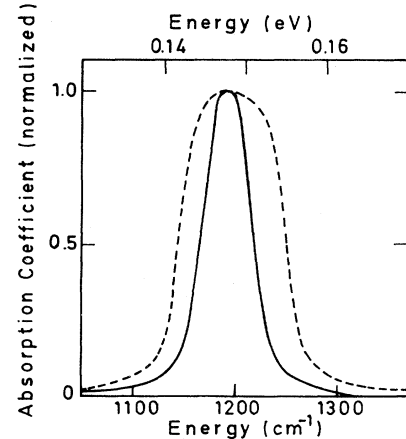


FIG. 3. Calculated intersubband spectra for a carrier temperature $T_c = 10$ K and an electron density of 4.2×10^{11} cm⁻² (solid line) and for hot electrons ($T_c = 350$ K, density 6.2×10^{11} cm⁻²).

represents a constant containing the dipole matrix element of the intersubband transition.

The solid line in Fig. 3 represents the absorption spectrum calculated for an electron density of $4.2 \times 10^{11} \text{ cm}^{-2}$ at 10 K. This band obtained with a Lorentzian profile $L(h\nu)$ of a full width at half maximum (FWHM) of 4 meV is in good agreement with the measured spectrum plotted in Fig. 1 (solid line). A significant change of the line shape results for an electron density of $6.2 \times 10^{11} \text{ cm}^{-2}$ and a carrier temperature of 350 K (dashed line in Fig. 3), i.e., the conditions of our picosecond experiments. The full half-width of the spectrum increases from 7 to approximately 13 meV with a slight shift of the line center to higher energies. These modifications are due to the following mechanisms: The $n=1$ and $n=2$ subbands get closer for increasing wave vector k_p and the energy ΔE_s of the intersubband transition decreases, i.e., an increase of the carrier temperature T_c at constant electron density results in a spectral broadening mainly to lower frequencies. However, band-gap renormalization by the additional electrons enlarges the separation of the subbands and shifts the transition to higher energies. As a result, there

is a well pronounced increase of oscillator strength at frequencies above the original absorption band. This finding as well as the calculated bandwidth agree with the experimental data of Fig. 1 (circles).

In summary, we have observed the distinct reshaping of the intersubband absorption spectrum of hot electrons in a MQW structure. Picosecond infrared spectroscopy directly reveals the broadening as well as the small spectral shift of the band with the transient carrier temperature. The changes of the spectral envelope are mainly due to the different dispersion of the two conduction subbands and the increase of the transition energy by band-gap renormalization. Thus the transient intersubband absorption is a sensitive probe of band structure and of many-body effects in a hot two-dimensional electron gas.

We would like to thank Professor W. Kaiser and Professor U. Rössler, Universität Regensburg, for numerous helpful discussions. Part of this work was sponsored by the Stiftung Volkswagenwerk and by the Bundesministerium für Forschung und Technologie of the Federal Republic of Germany.

*Present address: Dornier Medizintechnik GmbH, D-8034 Germering, Federal Republic of Germany.

†Present address: Physikalisches Institut der Universität Marburg, D-3550 Marburg, Federal Republic of Germany.

¹L. C. West and S. J. Eglash, *Appl. Phys. Lett.* **46**, 1156 (1985).

²B. F. Levine, K. K. Choi, C. G. Bethea, J. Walker, and R. J. Malik, *Appl. Phys. Lett.* **50**, 1092 (1987).

³M. Zachau, P. Hegelsen, F. Koch, D. Grützmacher, R. Mayer, and P. Balk, *Semicond. Sci. Technol.* **3**, 1029 (1988).

⁴P. von Allmen, M. Berz, F. K. Reinhart, and G. Harbeke, *Superlatt. Microstruct.* **5**, 259 (1989).

⁵H. Lobentanzer, W. König, W. Stolz, K. Ploog, T. Elsaesser, and R. J. Bäuerle, *Appl. Phys. Lett.* **53**, 571 (1988).

⁶R. J. Bäuerle, T. Elsaesser, W. Kaiser, H. Lobentanzer, W. Stolz, and K. Ploog, *Phys. Rev. B* **38**, 4307 (1988).

⁷T. Elsaesser, R. J. Bäuerle, W. Kaiser, H. Lobentanzer, W. Stolz, and K. Ploog, *Appl. Phys. Lett.* **54**, 256 (1989).

⁸T. Elsaesser, H. Lobentanzer, and A. Seilmeier, *Opt. Commun.* **52**, 355 (1985).

⁹F. A. Riddoch and B. K. Ridley, *J. Phys. C* **16**, 6971 (1983).

¹⁰H. Haug and S. W. Koch, *Phys. Rev. A* **39**, 1887 (1989).

¹¹J. A. Levenson, I. Abram, R. Raj, G. Dolique, J. L. Oudar, and F. Alexandre, *Phys. Rev. B* **38**, 13443 (1988).

¹²M. Braun and U. Rössler, *J. Phys. C* **18**, 3365 (1985); F. Malcher, G. Lommer, and U. Rössler, *Superlatt. Microstruct.* **2**, 267 (1986).

¹³U. Ekenberg, *Phys. Rev. B* **36**, 6152 (1987).

¹⁴W. Stolz, J. C. Maan, M. Altarelli, L. Tapfer, and K. Ploog, *Phys. Rev. B* **36**, 4301 (1987).